

# Muscle fibre recruitment can respond to the mechanics of the muscle contraction

James M. Wakeling<sup>1,\*</sup>, Katrin Uehli<sup>1</sup> and Antra I. Rozitis<sup>2</sup>

<sup>1</sup>*Structure and Motion Laboratory, Royal Veterinary College, Hawkshead Lane, North Mymms, Hatfield, Hertfordshire AL9 7TA, UK*

<sup>2</sup>*Human Performance Laboratory, Faculty of Kinesiology, University of Calgary, Calgary, Alberta T2N 1N4, Canada*

This study investigates the motor unit recruitment patterns between and within muscles of the triceps surae during cycling on a stationary ergometer at a range of pedal speeds and resistances. Muscle activity was measured from the soleus (SOL), medial gastrocnemius (MG) and lateral gastrocnemius (LG) using surface electromyography (EMG) and quantified using wavelet and principal component analysis. Muscle fascicle strain rates were quantified using ultrasonography, and the muscle–tendon unit lengths were calculated from the segmental kinematics. The EMG intensities showed that the body uses the SOL relatively more for the higher-force, lower-velocity contractions than the MG and LG. The EMG spectra showed a shift to higher frequencies at faster muscle fascicle strain rates for MG: these shifts were independent of the level of muscle activity, the locomotor load and the muscle fascicle strain. These results indicated that a selective recruitment of the faster motor units occurred within the MG muscle in response to the increasing muscle fascicle strain rates. This preferential recruitment of the faster fibres for the faster tasks indicates that in some circumstances motor unit recruitment during locomotion can match the contractile properties of the muscle fibres to the mechanical demands of the contraction.

**Keywords:** muscle; recruitment; fibre-type

## 1. INTRODUCTION

During locomotion, the skeletal muscles are excited by impulses from the  $\alpha$ -motorneurons that originate in the spinal cord. The excitability of the  $\alpha$ -motorneurons is related to the size of their cell bodies. The smallest  $\alpha$ -motorneurons have the lowest thresholds for excitation, and innervate the slowest muscle fibres. Thus, a weak stimulus to the motorneuron pool results in the slowest muscle fibres being recruited. The faster motor units are sequentially recruited as the stimulus strength increases in a graded fashion known as the size principle of motor unit recruitment (Henneman *et al.* 1965, 1974). The size principle has been a corner stone in our understanding of how different muscle fibres are used within a muscle. However, it predicts that slow muscle fibres will be used for fast contractions: a situation that is at odds with the contractile mechanics of the different fibre types.

Contractile properties of muscle fibres are related to the intrinsic speed  $\dot{\epsilon}_0$ , also known as the maximum unloaded strain rate, at which they can shorten. The shortening velocity at which the maximum mechanical power is generated (typically 0.25–0.36 $\dot{\epsilon}_0$ : Kushermick & Davies 1969; Swoap *et al.* 1997; He *et al.* 2000) and the velocity at which the maximum mechanical

efficiency is achieved (between 0.15 and 0.29 $\dot{\epsilon}_0$ ; Hill 1964; He *et al.* 2000) are both functions of  $\dot{\epsilon}_0$ . Therefore, generating mechanical power at a high efficiency is best achieved using faster muscle for faster contractions (Rome *et al.* 1988). However, preferential activation of fast fibres for fast tasks would contravene predictions made by the size principle. A number of studies have demonstrated situations, where the orderly recruitment of different muscle fibres can be reversed (e.g. Grimby & Hannerz 1977; Kanda *et al.* 1977; Hoffer *et al.* 1981; Nardone *et al.* 1989). Glycogen depletion studies have shown that fast fibres within the mixed vastus lateralis and gastrocnemius muscles in the bushbaby can be preferentially recruited during jumping as compared to running (Gillespie *et al.* 1974). However, it has yet to be established whether there are any general patterns which govern the preferential recruitment of faster muscle fibres over slower muscle fibres, and to what extent the fibre type recruitment is matched to the muscle shortening velocities during different movement tasks in a given muscle.

The myoelectric signals that are emitted from an active muscle contain information about the muscle fibre types that generated the signal. When a muscle is active, the faster fibres generate higher frequencies within the myoelectric spectra than slow fibres (Moritani *et al.* 1985; Gerdle *et al.* 1988; Solomonow *et al.* 1990; Elert *et al.* 1992; Kupa *et al.* 1995) and

\*Author for correspondence (jwakeling@rvc.ac.uk).

distinct high- and low-frequency bands have recently been identified that characterize activity from faster and slower fibres, respectively, in the rainbow trout, cat, rat and in man (Wakeling & Syme 2002; Wakeling *et al.* 2002; Wakeling & Rozitis 2004). Myoelectric signals with different frequencies but with the same power indicate the activity of different motor units and allow us to test whether there are distinct strategies of motor unit recruitment to match different locomotor demands.

In order to determine the extent to which faster muscle fibres may be preferentially recruited for fast contractions, we have related their recruitment patterns to muscle fascicle strain rates during cycling on an ergometer. The resistance of the ergometer was altered to vary the load on the legs, and the pedalling rate altered to vary the muscle fascicle strain rate. Activity patterns from the triceps surae muscle group were measured using electromyography (EMG), and a combination of wavelet decomposition and PC analysis of the EMG spectra was used to quantify spectral shifts. Ultrasound was used to directly visualize the changes in muscle fascicle length for each condition and kinematic measurement coupled to computer simulation used to estimate the muscle–tendon unit (MTU) lengths. We tested the hypothesis that EMG signals would shift to higher frequencies during locomotor tasks with higher muscle fascicle strain rates.

## 2. METHODS

### 2.1. Cycling

Six male cyclists (age  $31.0 \pm 2.1$  years; mass  $82.8 \pm 2.2$  kg; height  $1.90 \pm 0.01$  m) were tested at the Centre for Human Performance, Royal National Orthopaedic Hospital, Stanmore. Subjects gave their informed consent in accordance with the NHS Central Office for Research Ethics Committee. The subjects were either regular cyclists or classified as fit and used to cycling.

Subjects cycled with clipless pedals on an EC3200 ergometer (CatEye, Boulder, CO, USA) at a crank torque of 6.4 N m and a cadence of 60, 80, 100, 120 or 140 r.p.m. and additionally at a pedal cadence of 60 r.p.m. and a crank torque of 12, 17, 33, 39 or 44 N m. Each block of 10 experimental conditions was presented in a random order, and the blocks repeated three times.

An ultrasound scanner (HS-2000, Honda Electronics Co. Ltd, Japan) was used to image the muscle fascicles. The skin overlying the medial gastrocnemius (MG), the lateral gastrocnemius (LG) and the soleus (SOL), muscles of the right leg was shaved and coated with ultrasound gel. A 50 mm, 7.5 MHz, linear probe was placed over the gel and positioned to image muscle fascicles that were in the middle of the muscle belly, where the fascicle architecture is homogeneous (Maganaris *et al.* 1998) and in plane with the scanning image (Kawakami *et al.* 1993). For the SOL scans, the probe was positioned distal to the end of the gastrocnemius muscle belly so that dynamic shape changes in the gastrocnemius did not disrupt the image positioning of the ultrasound probe. A custom foam support

stabilized the probe and it was secured to the leg using elasticated bandage (Kawakami *et al.* 2002). The probe was moved between the muscles between each block of 10 experimental conditions. Ultrasound images were recorded directly onto digital videotape at 25 Hz and were recorded for 30 s for each condition. A 45 s rest period was given between trials. Three-dimensional segmental motion was simultaneously recorded for the thigh, shank, foot and pedal using active CODA markers (Charnwood Dynamics Ltd, Rothley, UK). For each tested muscle, the ultrasound and segmental positions were also recorded for a neutral condition with the subjects standing in their cycling shoes on the ground with feet flat and shoulder width apart and with the legs fully extended.

The test was repeated on a second day in order to measure the muscle activity. Bipolar surface EMG electrodes (12 mm diameter, 18 mm interelectrode distance; MA-300, Motion Lab Systems Inc., Baton Rouge, LA, USA) were placed on the muscle bellies of the MG, LG and SOL in the same place that the ultrasound scanner had been used after removal of the hair and cleaning with isopropyl wipes. After the bike was up to speed, data were recorded at 2000 Hz for 30 s.

### 2.2. Data analysis

Pedal cycles were identified when the right pedal passed through top dead centre, as determined by a motion analysis marker. The myoelectric signals were resolved into their intensities in time–frequency space using wavelet techniques (von Tscharner 2000). The intensity is a close approximation of the power of the signal contained within a given frequency band, and the intensity spectrum is equivalent to the power spectrum from the myoelectric signal. The total intensity and the EMG-intensity spectra were calculated for each of 25 pedal cycles. For each pedal cycle, the time was identified when the greatest total EMG-intensity occurred. The EMG intensities for each muscle and subject were normalized to the mean of the total intensities for all spectra across all trials. For each pedal cycle, two different windows were used to quantify the EMG-intensity spectra for further analysis: firstly, the mean intensity spectrum from the *whole cycle*, and secondly, the mean spectrum for the 100 ms *burst of activity* that occurred from  $-50$  to  $+50$  ms around the time of greatest EMG-intensity. Matrices of EMG-intensity spectra were compiled from the normalized spectra for all muscles and all subjects for the two types of windowed spectra. The PCs were calculated from the covariance matrices of the matrices of EMG-intensity spectra (figure 1a; Wakeling & Rozitis 2004). The PCs were calculated with no prior subtraction of the mean data and describe the components of the entire signal (Wakeling & Rozitis 2004). Each EMG-intensity spectrum can be reconstructed from the vector product of the PC weightings and the PC loading scores (figure 1b). The majority of the signal for any given myoelectric spectrum is defined by the first two PCs (PC I and PC II), and their relative loading scores give a measure of the frequency of the myoelectric signal (Wakeling 2004; Wakeling & Rozitis 2004).

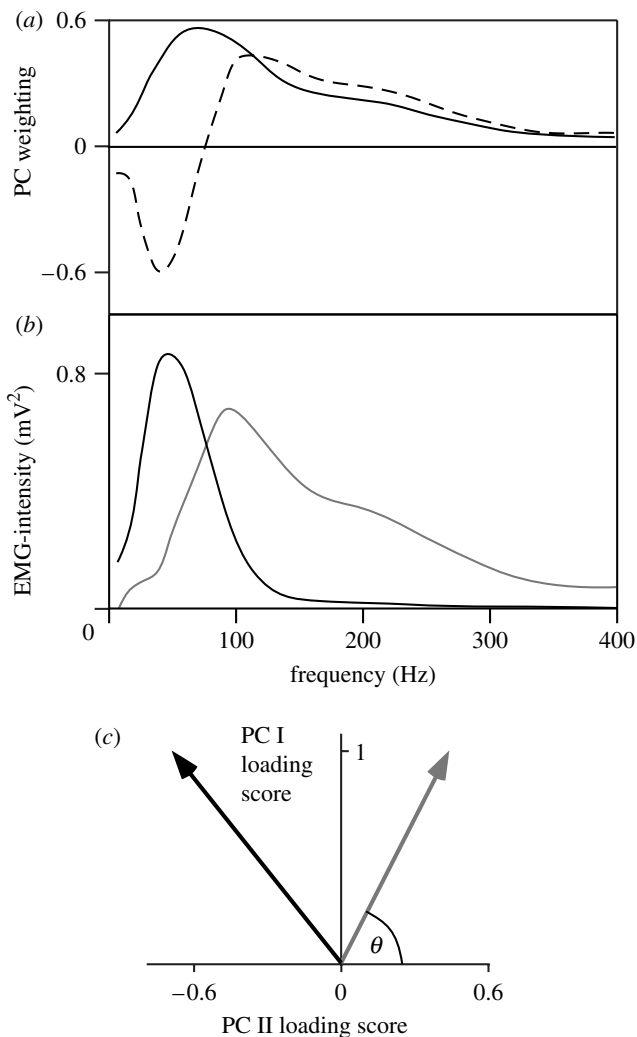


Figure 1. Principal component representation of EMG frequency spectra. (a) Principal component (PC) weightings for PC I (solid line) and PC II (dashed line) from the EMG-intensity spectra for six leg muscles (Wakeling & Rozitis 2004). (b) EMG-intensity spectra that can be reconstructed from vector products of the PC weightings shown in (a) with PC I + 0.45 PC II shown in grey and PC I - 0.69 PC II shown in black. (c) Vector representation of the spectra in (b) following the same colours as in (b) and indicating angle  $\theta$ .

The angle  $\theta$  was thus defined by the direction of the PC I-PC II loading score vector and used as a measure of the myoelectric frequency for each EMG-intensity spectrum (figure 1b,c).

The ultrasound images were digitized using NIH IMAGEJ 1.33 software (National Institutes for Health, USA). One hundred and fifty frames were digitized for each condition. For each frame, two points were digitized on the superficial aponeurosis echo, two on the deep aponeurosis echo and two on the echo of a muscle fascicle that appeared entirely within the scanning plane (figure 2). Where possible, the ends of the same muscle fascicle were tracked through the sequence of images for each condition. The coordinates were corrected for the aspect ratio error introduced during image acquisition and the fascicle length,  $l_f$ , calculated using linear interpolation. For each frame, the pennation angle was calculated as the angle between the muscle fascicle echo and the superficial

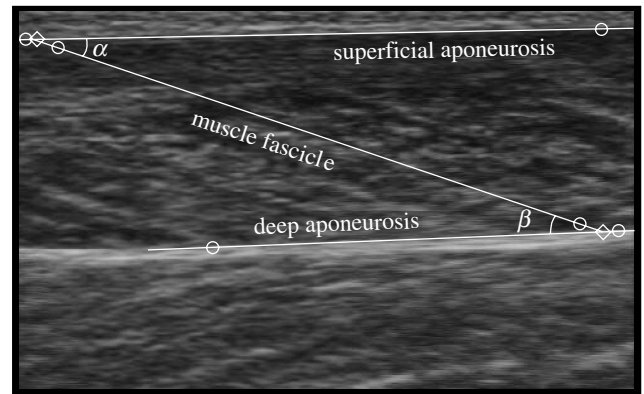


Figure 2. Ultrasound image from the medial gastrocnemius during cycling at a pedal speed of 60 r.p.m. and a crank torque of 17 N m. The circles show the digitized points, and the lines show the interpolated aponeurosis and fascicle trajectories. The diamonds show the ends of a muscle fascicle that has a pennation angle of  $\alpha$  with the superficial aponeurosis. The angle between the superficial and deep aponeuroses is  $\beta - \alpha$ .

aponeurosis echo (Maganaris *et al.* 1998), and the aponeurosis angle between the superficial and deep aponeuroses echo was also calculated (figure 2). The muscle fascicle length during the neutral trial represented the resting length,  $l_{f,0}$ , and was used to calculate the muscle fascicle strain,  $\varepsilon_f$ , during each cycling trial [ $\varepsilon_f = (l_f - l_{f,0}) / l_{f,0}$ ]. Least-squares minimization was used to fit a sinusoidal model [ $\varepsilon_f = k_1 + k_2 \sin(\gamma + \phi)$ ] to the muscle fascicle strain data for each trial, where  $k_1$ ,  $k_2$  and  $\gamma$  are fitted constants and  $\phi$  is the crank angle.

The sagittal plane knee and ankle joint angles recorded from the kinematics were used as input parameters to estimate the MTU length,  $l_{mtu}$ , for the SOL, MG and LG muscles using a graphics based software system: SIMM (Delp & Loan 1995) that was validated to a commonly used set of muscle coordinates (Brand *et al.* 1982). This package uses a set of empirical equations defining the musculoskeletal anatomy to calculate the position of the origin and insertion points of each muscle, and thus the MTU length, during each pedal cycle. The MTU length during the neutral trial was termed the resting length,  $l_{mtu,0}$ , and used to calculate the time-varying MTU strain,  $\varepsilon_{mtu}$ , for all cycles during each trial [ $\varepsilon_{mtu} = (l_{mtu} - l_{mtu,0}) / l_{mtu,0}$ ].

The strain rate,  $\dot{\varepsilon}$ , was calculated as the first time-derivative of strain. The maximum strain rate during shortening  $\dot{\varepsilon}_{max}$  is given by the magnitude of the minimum value of  $\dot{\varepsilon}$  for each cycle. The maximum strain rate for the muscle fascicles is described by the symbol  $\dot{\varepsilon}_{max,f}$ .

### 2.3. Statistics

The angle  $\theta$  is a measure of the major frequency content of the EMG-intensity spectra. Correlations between  $\theta$  and the crank torque, muscle fascicle strain rate and muscle fascicle strain were assessed using a general linear model analysis of covariance (MANCOVA) in which the subject identity and muscle were factors, and the crank torques,  $\dot{\varepsilon}_{max,f}$  and the mean fascicle strain for

Table 1. Muscle fascicle geometry from ultrasound measurements. (Values are given as mean  $\pm$  s.e.m. Angles were taken from the 10 cycles trials from each of the six subjects ( $n=60$ ). The fascicle lengths were determined during standing.)

muscle	aponeurosis angle ( $^{\circ}$ )	pennation angle ( $^{\circ}$ )	fascicle length (mm)
medial gastrocnemius	1.19 $\pm$ 0.12	21.31 $\pm$ 0.53	72.06 $\pm$ 3.55
lateral gastrocnemius	1.39 $\pm$ 0.12	15.73 $\pm$ 0.43	71.95 $\pm$ 5.65
soleus	1.13 $\pm$ 0.11	19.21 $\pm$ 0.57	79.89 $\pm$ 7.16

each sampling window were covariates (MINITAB v. 14, Minitab Inc., State College, PA). In order to test the hypothesis, we quantified whether  $\theta$  showed a significant, negative correlation with the muscle fascicle strain rate. All data are presented as mean  $\pm$  standard error of the mean (s.e.m.) and statistical tests were deemed significant at  $\alpha=0.05$ .

### 3. RESULTS

The geometric parameters for the muscle fascicles can be seen in table 1. The small aponeurosis angles confirmed that the imaged fascicles were in the central region of the muscle bellies. The mean pennation angles observed across all trials ranged between 15.7 and 21.3 $^{\circ}$  between the muscles. The mean strain excursion experienced across all conditions ranged between 12% for the MG and 20% for the SOL: analysis of variance showed that there was no significant effect of the pedal cadence on either the mean fascicle length or the fascicle strain for all three muscles.

The maximum muscle fascicle strain rates  $\dot{\epsilon}_{\max,f}$  during shortening correlated well with the predicted maximum MTU strain rates  $\dot{\epsilon}_{\max,mtu}$  during shortening for each set of trials. For the trials at a 6.4 N m crank torque but with an increasing pedalling cadence the two estimates of strain rate correlated with  $r^2=0.778$ , and for the trials at a 60 r.p.m. pedalling cadence and an increasing crank torque the two estimates of strain rate correlated with  $r^2=0.619$  for all subjects and muscles. The muscle fascicle strain rates were most similar to the MTU strain rates for the low torque trials but became relatively faster as the crank torque increased for all muscles. The muscle fascicle strain rates significantly increased with both the load and the cadence on the bicycle (figure 3). However, the total range of strain rates was greater for the increasing cadence test (2.8-, 2.2- and 2.2-fold) than for the increasing torque test (1.5-, 1.9- and 1.7-fold, for the MG, LG and SOL, respectively). The greatest values for  $\dot{\epsilon}_{\max,f}$  were  $0.94 \pm 0.17$ ,  $0.99 \pm 0.18$  and  $1.13 \pm 0.41$  s $^{-1}$  ( $n=6$  subjects) for the MG, LG and SOL, respectively.

The EMG-intensity calculated across the whole pedal cycles increased with both pedal torque and cadence (figure 4) for all three muscles. For any given mechanical power output on the ergometer, there was a greater EMG-intensity for the low torque–high cadence trials than for the high torque–low cadence trials. The

muscles varied the extent to which their activation was related to the pedal torques and cadence. The increases in EMG-intensity for the SOL in response to increased pedal torque were greater than for either gastrocnemius, while the increases in EMG-intensity for the SOL in response to increased cadence were less than for either of the gastrocnemii (figure 4).

Sample EMG signals from the LG for one subject are shown in figure 5 for three different trials. One pairing of these trials shares a common crank torque of 6.4 N m but at different cadences of 60 and 100 r.p.m.. A second pairing of these trials shares a common pedal cadence of 60 r.p.m. but at different crank torques of 6.4 and 44 N m during cycling. The raw EMG signals are delineated every time the pedal passes through top-dead centre: the traces show bursts of activity midway through each pedal cycle. Indeed, all three muscles were mainly activated during the concentric phases of each cycle and the time of maximum EMG-intensity was either not significantly different from the onset of muscle fascicle-shortening or occurred during the first half of shortening for most muscles and conditions (e.g. figure 6). The one exception to this was for the EMG-intensity for the LG for the trials at low torque but increasing cadence. For these trials, the maximum EMG-intensity occurred  $45 \pm 6.8$  ms before the start of muscle shortening.

PCs were calculated from the matrix of spectra for the 100 ms burst EMG-intensity spectra and from the EMG-intensity spectra for the entire pedal cycles. In both cases, the first two PCs of the EMG-intensity spectra described at least 88.1% of the EMG signal (figure 7a,b). The PC I loading scores correlated with the mean EMG-intensity for either the 100 ms burst or the entire pedal cycle with  $r^2 > 0.95$  ( $n \approx 12\,000$  spectra). The grey arrows in figure 7 show the direction of the PC I–PC II loading score vectors for the three extreme conditions (44 N m and 60 r.p.m., 6.4 N m and 60 r.p.m., 6.4 N m and 140 r.p.m.). The angles of the PC I–PC II loading score vectors,  $\theta$ , were smaller for the trials at the high pedal cadences than for the trials at high crank torques for the MG (figure 7a,b) and LG; this pattern was observed for both the 100 ms burst EMG-intensity spectra and from the EMG-intensity spectra for the entire pedal cycles. The decrease in  $\theta$  between the high torque–low cadence and low torque–high cadence trials for the MG corresponded to 32 and 17% increases in mean frequency of the EMG (as calculated from PC I and PC II) for the 100 ms burst and whole pedal cycle time windows, respectively (figure 7a,b). Both time windows showed trials with similar EMG-intensities (PC I loading score) but markedly different EMG-frequency composition (angle  $\theta$ ).

The MANCOVA tested whether the angle  $\theta$  correlated with either the crank torque, the muscle fascicle strain rate or the muscle fascicle strain (table 2). A significant negative correlation occurred between  $\theta$  and  $\dot{\epsilon}_{\max,f}$  when all the muscles were tested together, and this occurred for both the 100 ms bursts of activity and also for the entire pedal cycle. These correlations were independent of the covariance of either the crank torque or the muscle fascicle strain. The test was repeated using the data from individual

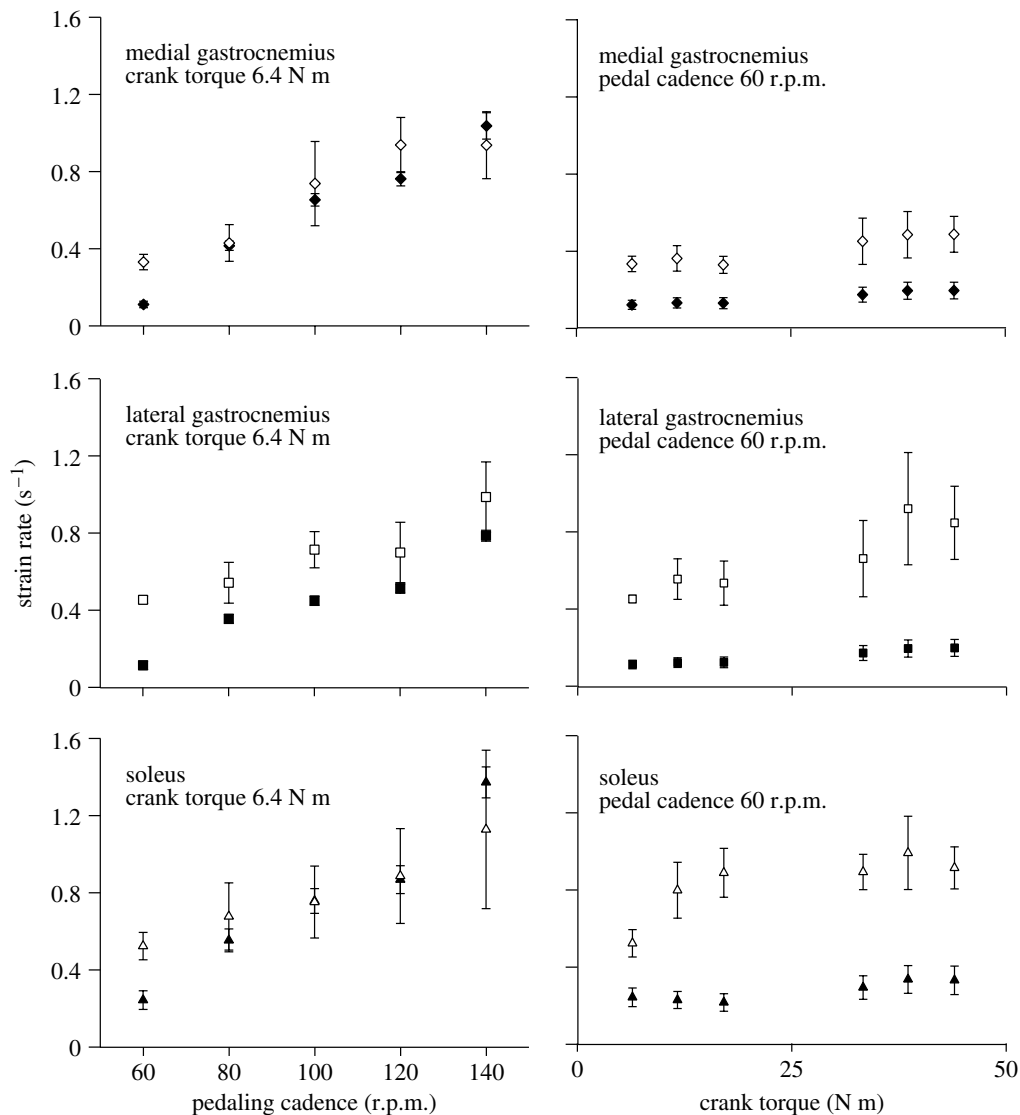


Figure 3. Maximum muscle strain rates during shortening as a function of pedal cadence and crank torque. Symbols show data for the medial gastrocnemius (diamond symbols), the lateral gastrocnemius (square symbols) and the soleus (triangle symbols). Muscle-tendon unit strain rates are shown by the filled symbols and muscle fascicle strain rates are shown by the open symbols. Points show the mean  $\pm$  s.e.m. for six subjects.

muscles, and  $\theta$  showed a significant negative correlation with  $\dot{\epsilon}_{\max,f}$  for the MG but not for the LG or SOL. The hypothesis that EMG signals would shift to higher frequencies for locomotor tasks with higher muscle fascicle strain rates during shortening was thus supported for the MG in this study.

#### 4. DISCUSSION

The experimental design was chosen to examine the recruitment patterns across a range of speeds and loads. The protocol was developed to independently vary the crank torque and the pedal cadence, however, the measured muscle fascicle strain rates were not totally decoupled from the crank torques. During the trials at the constant pedal cadence of 60 r.p.m. but with increasing crank torque, the predicted muscle-tendon strain rates showed no change with crank torque. These values were calculated from a geometrical model based on the skeletal orientation. However, the muscle fascicle strain rates increased with increasing crank

torque for these trials. This difference was, in part, due to the active nature of the muscle enabling it to stretch the tendons more at the higher loads, thus resulting in higher strain rates. Nonetheless, the greatest range in muscle fascicle strain rates was observed for the trials with increasing pedal cadence. The MG fascicle strain rates showed a greater relative change with increasing cadence and smaller relative change with increasing crank torque than for the LG or SOL (figure 3). Furthermore, the EMG-intensity for the MG appeared to be dominated relatively more by increases in pedal cadence than crank torque compared to the LG and SOL (figure 4). The MG thus responded more to the higher-velocity tasks, and it was also this muscle that showed the significant shifts to higher EMG frequencies with increasing fascicle strain rates (figure 7).

##### 4.1. Recruitment between muscles

The muscles of the triceps surae differ in both their structure and function. Both the MG and LG are two

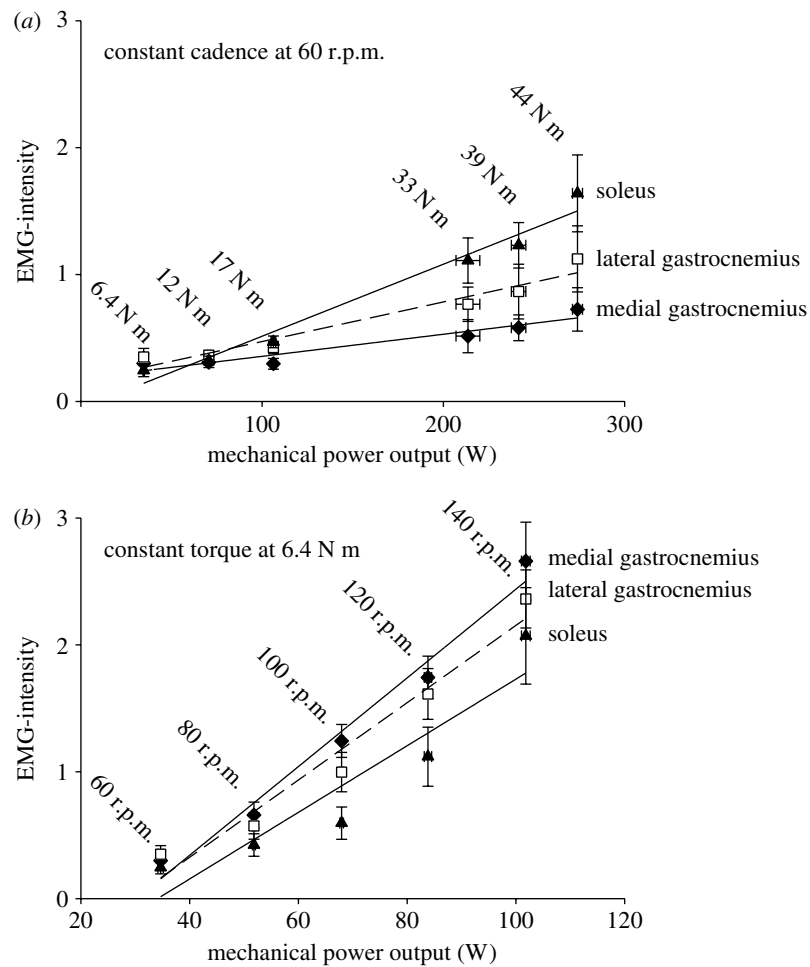


Figure 4. The total EMG-intensity per pedal cycle increased with both crank torque and pedal cadence. (a) Crank torque and (b) pedal cadence for the medial (diamond symbols) and lateral (square symbols) heads of the gastrocnemius and the soleus (triangle symbols). Points denote the mean  $\pm$  s.e.m. ( $n=450$  cycles).

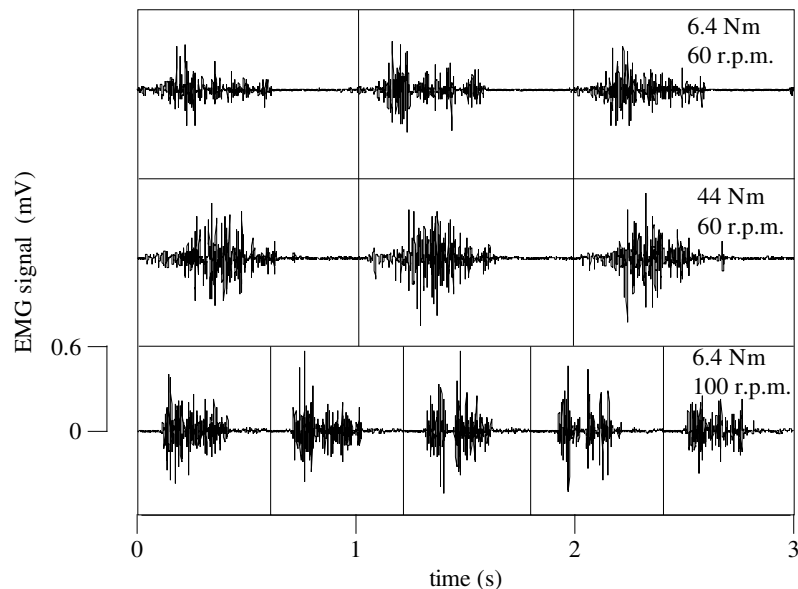


Figure 5. Electromyographic signals from the lateral gastrocnemius during cycling. Signals are shown from one subject for three different combinations of crank torque and pedal cadence. Raw signals with the top dead centre pedal position indicated by the vertical lines.

joint muscles with origins on the femoral epicondyles and both inserting at the posterior calcaneus via the Achilles tendon. These muscles span both the knee and ankle joints. The SOL, on the other hand, is a one joint

muscle with its origin on the head of the posterior tibia and fibula and inserting at the calcaneus via the Achilles tendon. All three of these muscles share the common role of ankle plantarflexion. During the cycling

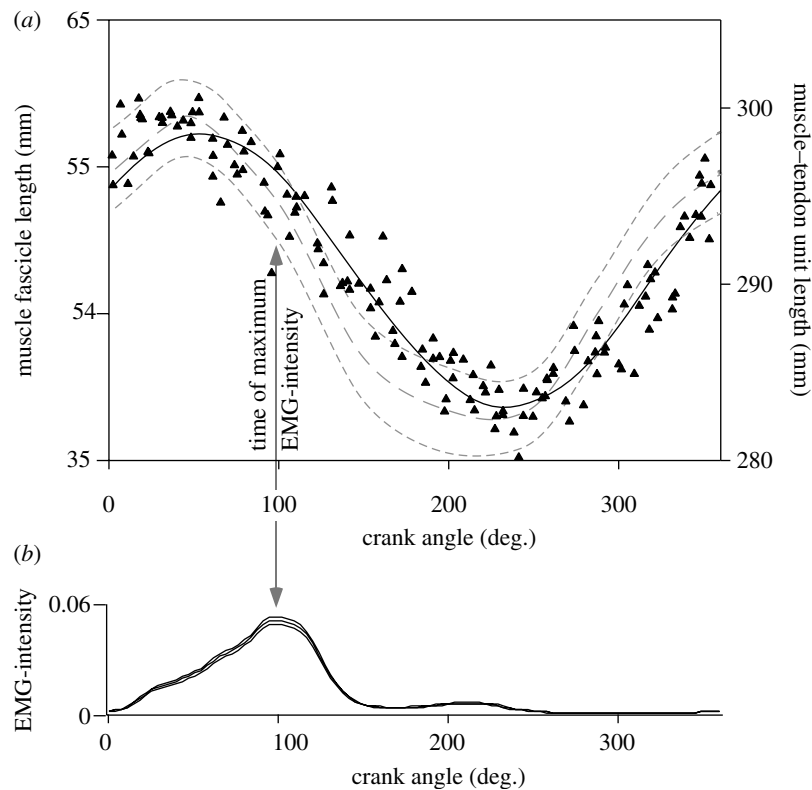


Figure 6. Muscle lengths and activity pattern for the soleus during cycling at a pedal cadence of 60 r.p.m. against a load of 33 N m. (a) Muscle fascicle lengths measured by ultrasound for one subject are shown by the triangles. The modelled muscle fascicle length is shown by the solid black line,  $r^2=0.907$ . The modelled muscle-tendon unit length is shown by the grey dashed lines (mean  $\pm$  s.e.m. for all six subjects). (b) Normalized EMG-intensity for the soleus during cycling at a cadence of 60 r.p.m. against a load of 33 N m. Intensity is shown as mean  $\pm$  s.e.m. for all six subjects ( $n=450$  cycles).

trials in this study ankle plantar flexion occurred between pedal angles of approximately 30–180°. Variation also occurs in the internal structure of these muscles with a difference in muscle fascicle pennation angles (table 1), and in muscle fibre-type composition. In man, the SOL muscle contains significantly more (88%) slow, type I, muscle fibres than the MG (51%) and LG (47%) (Johnson *et al.* 1973).

Studies in the cat have shown that recruitment is distributed between the muscles of the triceps surae in a manner that depends on the mechanical task. The paw-shake is a high-frequency (up to 12 Hz) cycle of ankle flexion-extensions. In the cat, the SOL contains almost entirely slow fibres, and this muscle is not activated during the fastest paw-shakes (Smith *et al.* 1980). It has been argued that the slower activation and relaxation kinetics of the slow fibres in the SOL preclude it from producing useful force during this activity, therefore requiring the paw-shakes to be driven by the LG (Smith & Spector 1981). On the other hand, the SOL shows relatively greater EMG than the MG for slower and less intense activities (Kaya *et al.* 2003).

In this study, we also observed the SOL playing a relatively greater role in the slower contractions than in the faster contractions (figure 4). The relationships between EMG-intensity and mechanical power output at the crank showed that the SOL was most responsive to increases in crank torque, while the MG was most responsive to increases in pedal cadence and thus strain rate.

#### 4.2. Recruitment within muscles

A major finding from this study was the shift to higher EMG frequencies at the faster muscle fascicle strain rates for the MG (figure 7). Many studies quantify EMG frequencies by the mean or median frequency of the EMG power spectra (Roy *et al.* 1986; Solomonow *et al.* 1990; Kupa *et al.* 1995; De Luca 1997). However, in the current study, the shift in frequency does not merely represent an increase in the mean frequency of the EMG-intensity spectrum but more specifically occurs as a decrease in the low-frequency (less than 100 Hz) components and an increase in the high-frequency (greater than 100 Hz) components of the spectra (Wakeling & Rozitis 2004). Furthermore, the results showed that shifts in frequency occurred even when the total EMG-intensity remained the same and the statistical analysis showed that the strain rate-dependent shifts in frequency occurred independently from changes in the locomotor load, measured as crank torque and the muscle fascicle strain.

There are many factors that can affect the interpretation of an EMG signal. However, careful design and interpretation of the experiment can reduce the number of factors that influence the major results. This study is unique in that it combined direct observations of the muscle fascicles using ultrasonography coupled to recordings from those fascicles using EMG. Therefore, we can address the speculation and assumptions typically encountered when interpreting EMG: (i) Prolonged changes in the muscle fatigue status can

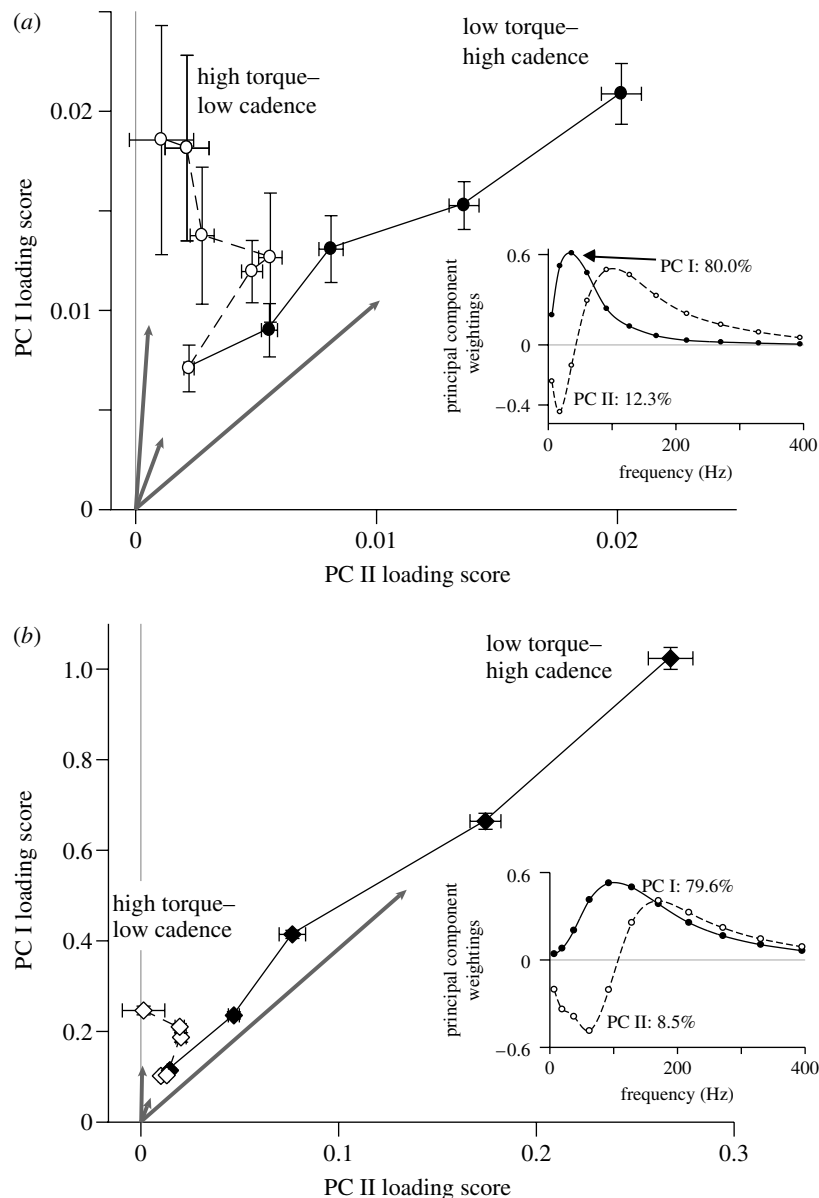


Figure 7. Principal component representation of the EMG-intensity spectra during cycling at a range of pedal cadences and crank torques for the medial gastrocnemius. (a) Principal components describing the 100 ms bursts of muscle activity centred around the time of maximum EMG-intensity. (b) Principal components describing the total EMG-intensity across each pedal cycle. The principal components were calculated from EMG spectra from all three muscles tested. The loading score panels show the mean  $\pm$  s.e.m. ( $n=450$  cycles) loading scores for the first two principal components: trials with low crank torque and increasing pedal cadence are shown with solid symbols and solid lines and trials with low pedal cadence and increasing crank torque are shown with open symbols and dashed lines. Vectors from the origin to the three extreme points are shown by the grey arrows. The inset panels show the first two principal component weighting spectra PC I (solid line) and PC II (dashed line).

decrease the EMG frequencies (Petrofsky 1979) while increases in temperature that occur with exercise (Saltin *et al.* 1968) can increase the EMG frequency (Stålberg 1966). However, the randomized block design of the experimental protocol removed bias in the results that would otherwise have been caused by these gradual and sustained effects. (ii) Muscle fibre length affects the frequency of an EMG signal with lower frequencies being generated from longer fibres (Doud & Walsh 1995). In this study, we directly imaged the muscle fascicle strains and incorporated them as factors into the EMG analysis. When muscle fascicle strain was included as a covariate in the MANCOVA (table 2), the results showed that there was no significant effect of the fascicle strain on the angle  $\theta$  for either all the muscles

pooled together or more specifically for the MG tested on its own. (iii) Non-propagating cross-talk between muscles can introduce higher-frequency components into the EMG-intensity spectra (Farina *et al.* 2002). This high-frequency artefact increases with signal amplitude but reaches less than 1% of the maximum EMG-intensity (for a double-differential recording with an interelectrode distance of 20 mm, comparable to the recordings in this study: Farina *et al.* 2002). Furthermore, in the current study, decreases in  $\theta$  are observed between trials for the MG even when the LG EMG-intensity decreased, and vice versa, and these effects are opposite to those that would be observed during the presence of cross-talk. (iv) Variation in the depth of the motor units within the muscle can alter the frequency

Table 2. The effect of mechanical variables on the angle  $\theta$ . (Values are the probabilities that the variables significantly covary with  $\theta$  (from the MANCOVAs). The arrows denote the direction of the association:  $\uparrow$  positive and  $\downarrow$  negative, when the covariates are significant ( $p < 0.05$ .)

covariate	all muscles		medial gastrocnemius	
	100 ms burst	Whole cycle	100 ms burst	whole cycle
crank torque	0.080	<0.001 $\uparrow$	0.792	<0.001 $\uparrow$
muscle fascicle strain rate	0.009 $\downarrow$	<0.001 $\downarrow$	<0.001 $\downarrow$	<0.001 $\downarrow$
muscle fascicle strain	0.224	0.892	0.219	0.300

content of their recorded spectra, with deeper fibres generating lower frequency spectra. The effects of motor unit depth on recorded EMG signals can be predicted using volume conductor models (Roeveland *et al.* 1997; Block *et al.* 2002). One such model can be downloaded from the Internet (Block *et al.* 2002) and predicts that shifts in EMG frequency, similar to those between the extreme conditions in figure 7, can be generated by fast motor units (conduction velocity  $4.7 \text{ m s}^{-1}$ ) at a depth of 5 and 15 mm from the skin surface. However, attenuation with depth means that the EMG recorded from the 15 mm deep motor unit would have a total intensity less than 1% of that from the more superficial unit. On the other hand, a superficial motor unit with a reduced conduction velocity ( $1.6 \text{ m s}^{-1}$ : slower fibres) could produce the lower-frequency spectrum with similar EMG-intensity to that of a superficial fast motor unit (Block *et al.* 2002). However, the ultrasound images showed that the fascicles all spanned the superficial and deep aponeuroses in the muscle bellies from where the recordings were made (figure 2). This layer of muscle extended to a depth of 20–25 mm (data in table 1) from the skin and so contributed to the significant majority of the EMG signal. Each fascicle and motor unit extended to the superficial aponeurosis and there was no evidence of any populations of deep motor units within this layer. The spectral shifts to higher EMG frequencies at the faster pedal cadences (figure 7) are thus not the result from activity from different populations of motor units at different depths within the muscle.

It is commonly speculated that higher EMG frequencies are generated from faster muscle fibres due to their larger diameter. However, we do not know of any experimental evidence that supports these claims *in vivo*. On the other hand, theory predicts that the conduction velocity of the motor unit action potentials should change with altered electrical properties of the sarcolemmas (Hodgkin 1954) and these are known to vary between fast and slow muscle fibre types in mammals (Luff & Atwood 1972). The evidence suggests that the higher conduction velocity, and associated EMG frequency, observed in the faster fibres

occurs independently of any difference in muscle fibre diameter (Buchthal *et al.* 1955; Gerdle *et al.* 2000; Wakeling *et al.* 2002).

The observation of different spectral frequencies at similar EMG-intensities is an indicator that different populations of motor units are being recruited for the different trials and has previously been reported for running (Wakeling 2004). Faster motor units have higher conduction velocities for their motor unit action potentials than slow motor units (Sadoyama *et al.* 1988; Kupa *et al.* 1995; Wakeling & Syme 2002) due to differences in the electrical properties of the sarcolemma. Recently, we have reported that distinct EMG frequency bands can characterize activity from different types of muscle fibre across a range of species and recording systems (Wakeling & Syme 2002; Wakeling *et al.* 2002; Wakeling & Rozitis 2004). The faster motor units typically generate EMG spectra with centre-frequencies 2–3 times higher than those from slower motor units. The PC analysis of the spectra quantifies an angle  $\theta$  that is a direct measure of this frequency shift and has previously been shown to discriminate the activity of different types of motor unit within the SOL in man (Wakeling & Rozitis 2004). The fibres in mixed muscle may exhibit a continuum of mechanical and biochemical properties from the fastest to the slowest, but the analysis techniques used here are capable of quantifying shifts in EMG frequency along such a continuum (Wakeling 2004). The results from these cycling tests show that decreases in  $\theta$  are significantly related to increases in the muscle fascicle strain rate for the MG. These results indicate that one factor that can lead to the preferential recruitment of faster motor units is rapid shortening velocity of the muscle fascicles.

#### 4.3. Motor control during locomotion

It is traditionally assumed that the basic plan for the recruitment of different types of muscle fibre stems from the ‘size principle’ of motor recruitment (Henneman *et al.* 1965, 1974) where the smallest  $\alpha$ -motorneurons are the most excitable within the spinal cord. These motorneurons, in turn, innervate the motor units containing the slowest muscle fibres. There are a number of facilitatory and inhibitory neural pathways coupled to a range of interneurons within the spinal cord that can alter the recruitment patterns. Of particular note are the Renshaw cells that regulate the firing rate of the  $\alpha$ -motorneurons and are more strongly excited by the collaterals of large motorneurons than small ones (Ryall *et al.* 1972; Hultborn *et al.* 1988a). Recurrent inhibition from the Renshaw cells causes a disfacilitatory influence on the already active, slower motor units when faster motor units are recruited (Friedman *et al.* 1981; Broman *et al.* 1985; Hultborn *et al.* 1988b). Renshaw cells thus provide a mechanism by which size principle type recruitment patterns may be reversed.

The size principle makes the specific predictions that low intensity contractions use the slowest motor units and that the fast motor units can only be recruited when all the slower motor units have already been activated. However, exceptions to this pattern have

been recorded for a number of different species and activities (e.g. Basmajian 1963; Wagman *et al.* 1965; Gillespie *et al.* 1974; Grimby & Hannerz 1977; Kanda *et al.* 1977; Stephens *et al.* 1978; Hoffer *et al.* 1981; Nardone *et al.* 1989; Wakeling 2004). It remains an interesting problem as to how and why different populations of motor units are used for different movement tasks. The different types of motor units have different mechanical properties and it is possible that selective motor recruitment is a means by which the different types of unit are recruited according to the mechanical demands on the whole muscle. Interestingly, a study of the total EMG activity of the quadriceps muscles during cycling at a range of pedalling cadences, but at a fixed load, has led to the speculation that preferential recruitment of the faster muscle fibres would occur at the faster speeds during locomotion in man (Citterio & Agostoni 1984). Our study provides data that support this speculation. The preferential recruitment of the faster motor units in MG is partially related to the strain rate of the muscle fascicles.

It has previously been suggested that muscles that are too slow to power a movement will not be activated; this occurs between the fast and slow compartments of the myotomal muscle of fast-starting fish (Rome *et al.* 1988), and between the SOL and gastrocnemii of the cat during paw-shaking (Smith & Spector 1981). The preferential recruitment of faster motor units within a mixed muscle for faster activities would follow these mechanical arguments and, indeed, preferential recruitment of the faster fibres in the vastus lateralis and gastrocnemius muscles of the bushbaby (*Galago senegalensis*) has been observed during jumping as opposed to running (Gillespie *et al.* 1974). The muscle strain rates were not recorded in the bushbaby study and it is not known whether they exceeded the intrinsic speeds of the slower fibres. However, it is likely that strain rates do not exceed the slow fibre maxima for many moderate locomotor activities and it has been suggested that in man the intrinsic speeds of the slow fibres may never be exceeded (Bottinelli & Reggiani 2000). There is some debate as to the intrinsic speed, maximum unloaded strain rate  $\dot{\epsilon}_0$ , for human muscle fibres *in vivo*. Measurements from isolated bundles of muscle at body temperature have reported intrinsic speeds of 2 and 6 s<sup>-1</sup> for slow and fast human muscle fibres, respectively (Faulkner *et al.* 1986), although it has been argued that these values could be less than 6 s<sup>-1</sup> and greater than 14 s<sup>-1</sup>, respectively (Epstein & Herzog 1998). The greatest  $\dot{\epsilon}_{\max,f}$  observed in this study was  $1.1 \pm 0.4$  s<sup>-1</sup> and is less than even the most conservative estimate for slow fibre intrinsic speeds. Therefore, the preferential recruitment observed in this experiment occurred when it may have been mechanically beneficial but it certainly was not necessary. However, it should be noted that two of the six subjects achieved maximum strain rates in excess of 2 s<sup>-1</sup> (2.10 and 2.70 s<sup>-1</sup>) and so it is possible that fast activities in man may reach or even exceed the maximum intrinsic speeds of the slower muscle fibres. The strain rates that achieve maximum mechanical power output are typically assumed to be between 0.25 and 0.36  $\dot{\epsilon}_0$  (Kushermick & Davies 1969;

Swoap *et al.* 1997; He *et al.* 2000) and it is interesting to note that the  $\dot{\epsilon}_{\max,f}$  from this study may have reached 0.47  $\dot{\epsilon}_0$  for the slow fibres in the MG (according to  $\dot{\epsilon}_{\max,f}=0.94$  and  $\dot{\epsilon}_0=2$  for slow fibres; Faulkner *et al.* 1986). It is possible that the shift in recruitment to the faster fibres in MG was a response to place the active fibres at strain rates where they could achieve greater power outputs.

The results from this study support previous observations that different motor units may be recruited in a task-specific fashion during locomotion. We now additionally show that under certain cyclical locomotor conditions the recruitment patterns of different types of motor unit are related to the mechanical requirements of the locomotor task. This preferential recruitment can occur across a range of locomotor speeds and indeed even occurs at the speeds where the slower fibres could still produce useful force.

We thank the Motion Analysis Laboratory at the Royal National Orthopaedic Hospital, Stanmore for use of their facilities, John Hutchinson and Emma Tole for help and discussions, Martin Sheldon for the loan of the ultrasound scanner and NSERC of Canada for funding.

## REFERENCES

- Basmajian, J. V. 1963 Control and training of individual motor units. *Science* **141**, 440–441.
- Block, J. H., Stegeman, D. F. & van Oosterom, A. 2002 Three-layer volume conductor model and software package for applications in surface electromyography. *Ann. Biomed. Eng.* **30**, 566–577. (doi:10.1114/1.1475345)
- Bottinelli, R. & Reggiani, C. 2000 Human skeletal muscle fibres: molecular and functional diversity. *Prog. Biophys. Mol. Biol.* **73**, 195–262. (doi:10.1016/S0079-6107(00)00006-7)
- Brand, R. A., Crowninshield, R. D., Wittstock, C. E., Pederson, D. R., Clark, C. R. & van Krieken, F. M. 1982 A model of the lower extremity muscular anatomy. *J. Biomech. Eng.* **104**, 304–310.
- Broman, H., De Luca, C. J. & Mambrito, B. 1985 Motor unit recruitment and firing rates interaction in the control of human muscles. *Brain Res.* **337**, 311–319. (doi:10.1016/0006-8993(85)90068-X)
- Buchthal, F., Guld, C. & Rosenfalck, P. 1955 Innervation zone and propagation velocity in human muscle. *Acta Physiol. Scand.* **35**, 174–190.
- Citterio, G. & Agostoni, E. 1984 Selective activation of quadriceps muscle fibers according to bicycling rate. *J. Appl. Physiol.* **57**, 371–379.
- De Luca, C. J. 1997 The use of surface electromyography in biomechanics. *J. Appl. Biomech.* **13**, 135–163.
- Delp, S. L. & Loan, J. P. 1995 A graphics-based software system to develop and analyze models of musculoskeletal structures. *Comput. Biol. Med.* **25**, 21–34. (doi:10.1016/0010-4825(95)98882-E)
- Doud, J. R. & Walsh, J. M. 1995 Muscle fatigue and muscle length interaction: effect on the EMG frequency components. *Electromyogr. Clin. Neurophysiol.* **35**, 331–339.
- Elert, J., Rantapää-Dahlqvist, S. B., Henriksson-Larsén, K., Lorentzon, R. & Gerdtle, B. U. C. 1992 Muscle performance electromyography and fibre type composition in fibromyalgia and work-related myalgia. *Scand. J. Rheumatol.* **21**, 29–34.

- Epstein, M. & Herzog, W. 1998 *Theoretical models of skeletal muscle. Biological and mathematical considerations*. New York: Wiley.
- Farina, D., Merletti, R., Indino, B., Nazzaro, M. & Pozzo, M. 2002 Surface EMG crosstalk between knee extensor muscles: experimental and model results. *Muscle Nerve* **26**, 681–695. (doi:10.1002/mus.10256)
- Faulkner, J. A., Claffin, D. R. & McCully, K. K. 1986 Power output of fast and slow fibers from human skeletal muscles. In *Human muscle power* (ed. N. L. Jones, N. McCartney & A. J. Comas), pp. 81–94. Champaign, IL: Human Kinetics Publishers Inc.
- Friedman, W. A., Sypert, G. W., Munson, J. B. & Fleshman, J. W. 1981 Recurrent inhibition in type-identified motoneurons. *J. Neurophysiol.* **46**, 1349–1359.
- Gerdle, B., Wretling, M.-L. & Henriksson-Larsén, K. 1988 Do the fibre-type proportion and the angular velocity influence the mean power frequency of the electromyogram? *Acta Physiol. Scand.* **134**, 341–346.
- Gerdle, B., Karlsson, S., Crenshaw, A. G., Elert, J. & Fridén, J. 2000 The influences of muscle fibre proportions and areas upon EMG during maximal dynamic knee extensions. *Eur. J. Appl. Physiol.* **81**, 2–10.
- Gillespie, C. A., Simpson, D. R. & Edgerton, V. R. 1974 Motor unit recruitment as reflected by muscle fibre glycogen loss in a prosimian (bushbaby) after running and jumping. *J. Neurol. Neurosurg. Psychiatry* **37**, 817–824.
- Grimby, L. & Hannerz, J. 1977 Firing rate and recruitment order of toe extensor motor units in different modes of voluntary contraction. *J. Physiol.* **264**, 865–879.
- He, Z.-H., Bottinelli, R., Pellegrino, M. A., Ferenczi, M. A. & Reggiani, C. 2000 ATP consumption and efficiency of human single muscle fibers with different myosin isoform composition. *Biophys. J.* **79**, 945–961.
- Henneman, E., Somjen, G. & Carpenter, D. O. 1965 Functional significance of cell size in spinal motoneurons. *J. Neurophysiol.* **28**, 560–582.
- Henneman, E., Clamann, H. P., Gillies, J. D. & Skinner, R. D. 1974 Rank order of motoneurons within a pool, law of combination. *J. Neurophysiol.* **37**, 1338–1349.
- Hill, A. V. 1964 The efficiency of mechanical power development during muscular shortening and its relation to load. *Proc. R. Soc. B* **159**, 319–324.
- Hodgkin, A. L. 1954 A note on conduction velocity. *J. Physiol.* **125**, 221–224.
- Hoffer, J. A., O'Donovan, M. J., Pratt, C. A. & Loeb, G. E. 1981 Discharge patterns in hindlimb motoneurons during normal cat locomotion. *Science* **213**, 466–468.
- Hultborn, H., Katz, R. & Mackel, R. 1988a Distribution of recurrent inhibition within a motor nucleus. II. Amount of recurrent inhibition in motoneurons to fast and slow units. *Acta Physiol. Scand.* **134**, 363–374.
- Hultborn, H., Lipski, J., Mackel, R. & Wigström, H. 1988b Distribution of recurrent inhibition within a motor nucleus. I. Contribution from slow and fast motor units to the excitation of Renshaw cells. *Acta Physiol. Scand.* **134**, 347–361.
- Johnson, M. A., Polgar, J., Weightman, D. & Appleton, D. 1973 Data on the distribution of fibre types in thirty-six human muscles. An autopsy study. *J. Neurol. Sci.* **18**, 111–129. (doi:10.1016/0022-510X(73)90023-3)
- Kanda, K., Burke, R. E. & Walmsley, B. 1977 Differential control of fast and slow twitch motor units in the decerebrate cat. *Exp. Brain Res.* **29**, 57–74. (doi:10.1007/BF00236875)
- Kawakami, Y., Abe, T. & Fukunaga, T. 1993 Muscle-fiber pennation angles are greater in hypertrophied than in normal muscles. *J. Appl. Physiol.* **74**, 2740–2744.
- Kawakami, Y., Muraoka, T., Ito, S., Kanehisa, H. & Fukunaga, T. 2002 *In vivo* muscle fibre behaviour during counter movement exercise in humans reveals a significant role for tendon elasticity. *J. Physiol.* **540**, 635–646. (doi:10.1113/jphysiol.2001.013459)
- Kaya, M., Leonard, T. & Herzog, W. 2003 Coordination of medial gastrocnemius and soleus forces during cat locomotion. *J. Exp. Biol.* **206**, 3645–3655. (doi:10.1242/jeb.00544)
- Kupa, E. J., Roy, S. H., Kandarian, S. C. & de Luca, C. J. 1995 Effects of muscle fibre type and size on EMG median frequency and conduction velocity. *J. Appl. Physiol.* **79**, 23–32.
- Kushermick, M. J. & Davies, R. E. 1969 The chemical energetics of muscle contraction. II. The chemistry, efficiency and power of maximally working sartorius muscles. *Proc. R. Soc. B* **174**, 315–353.
- Luff, A. R. & Atwood, H. L. 1972 Membrane properties and contraction of single muscle fibres in the mouse. *Am. J. Physiol.* **222**, 1435–1440.
- Maganaris, C. N., Baltzopoulos, V. & Sargeant, A. J. 1998 *In vivo* measurements of the triceps surae complex architecture in man: implications for muscle function. *J. Physiol.* **512**, 603–614. (doi:10.1111/j.1469-7793.1998.603be.x)
- Moritani, T., Gaffney, F. D., Carmichael, T. & Hargis, J. 1985 Interrelationships among muscle fibre types, electromyogram and blood pressure during fatiguing isometric contraction. In *Biomechanics*, vol. IXA, (ed. D. A. Winter, R. W. Norman, R. P. Wells, K. C. Hayes & A. E. Patla). International series on biomechanics, pp. 287–292. Champaign, IL: Human Kinetics Publishers Inc.
- Nardone, A., Romanò, C. & Schieppati, M. 1989 Selective recruitment of high-threshold human motor units during voluntary isotonic lengthening of active muscles. *J. Physiol.* **409**, 451–471.
- Petrofsky, J. S. 1979 Frequency and amplitude analysis of the EMG during exercise on the bicycle ergometer. *Eur. J. Appl. Physiol.* **41**, 1–15. (doi:10.1007/BF00424464)
- Roeleveld, K., Blok, J. H., Stegeman, D. F. & van Oosterom, A. 1997 Volume conduction models for surface EMG: confrontation with measurements. *J. Electromyogr. Kinesiol.* **7**, 221–232. (doi:10.1016/S1050-6411(97)00009-6)
- Rome, L. C., Funke, R. P., Alexander, R. McN., Lutz, G., Aldridge, H., Scott, F. & Freadman, M. 1988 Why animals have different muscle fibre types. *Nature* **335**, 824–827. (doi:10.1038/335824a0)
- Roy, S. H., de Luca, C. J. & Schneider, J. 1986 Effects of electrode location on myoelectric conduction velocity and median frequency estimates. *J. Appl. Physiol.* **61**, 1510–1517.
- Ryall, R. W., Piercey, M. F., Polosa, C. & Goldfarb, J. 1972 Excitation of Renshaw cells in relation to orthodromic and antidromic excitation of motoneurons. *J. Neurophysiol.* **35**, 137–148.
- Sadoyama, T., Masuda, T., Miyata, H. & Katsuta, S. 1988 Fibre conduction velocity and fibre composition in human vastus lateralis. *Eur. J. Appl. Physiol.* **57**, 767–771. (doi:10.1007/BF01076001)
- Saltin, B., Gagge, A. P. & Stolwijk, J. A. J. 1968 Muscle temperature during submaximal exercise in man. *J. Appl. Physiol.* **25**, 679–688.
- Smith, J. L. & Spector, S. A. 1981 Unique contributions of slow and fast extensor muscles to the control of limb movements. In *Motor unit types, recruitment and plasticity in health and disease*, vol. 9, (ed. J. E. Desmedt) Progress in clinical neurophysiology, pp. 161–175. Basel: Karger.
- Smith, J. L., Betts, B., Edgerton, V. R. & Zernicke, R. F. 1980 Rapid ankle extension during paw shakes: selective

- recruitment of fast ankle extensors. *J. Neurophysiol.* **43**, 612–620.
- Solomonow, M., Baten, C., Smit, J., Baratta, R., Hermens, H., D'Ambrosia, R. & Shoji, H. 1990 Electromyogram power spectra frequencies associated with motor unit recruitment strategies. *J. Appl. Physiol.* **68**, 1177–1185.
- Stålberg, E. 1966 Propagation velocity in human muscle fibres *in situ*. *Acta Physiol. Scand.* **70**, 3–112.
- Stephens, J. A., Garnett, R. & Buller, N. P. 1978 Reversal of recruitment order of single motor units produced by cutaneous stimulation during voluntary muscle contraction in man. *Nature* **272**, 362–364. (doi:10.1038/272362a0)
- Swoap, S. J., Caiozzo, V. J. & Baldwin, K. M. 1997 Optimal shortening velocities for *in situ* power production of rat soleus and plantaris muscles. *Am. J. Physiol.* **273**, C1057–C1063.
- von Tscharnar, V. 2000 Intensity analysis in time–frequency space of surface myoelectric signals by wavelets of specified resolution. *J. Electromyogr. Kinesiol.* **10**, 433–445. (doi:10.1016/S1050-6411(00)00030-4)
- Wagman, I. H., Pierce, D. S. & Burger, R. E. 1965 Proprioceptive influence in volitional control of individual motor units. *Nature* **207**, 957–958.
- Wakeling, J. M. 2004 Motor units are recruited in a task dependent fashion during locomotion. *J. Exp. Biol.* **207**, 3883–3890. (doi:10.1242/jeb.01223)
- Wakeling, J. M. & Rozitis, A. I. 2004 Spectral properties of myoelectric signals from different motor units distinguished during ramped contractions of the leg extensors. *J. Exp. Biol.* **207**, 2519–2528. (doi:10.1242/jeb.01042)
- Wakeling, J. M. & Syme, D. A. 2002 Wave properties of action potentials from fast and slow motor units of rats. *Muscle Nerve* **26**, 659–668. (doi:10.1002/mus.10263)
- Wakeling, J. M., Kaya, M., Temple, G. K., Johnston, I. A. & Herzog, W. 2002 Determining patterns of motor recruitment during locomotion. *J. Exp. Biol.* **205**, 359–369.